Land intercalibration and drift monitoring of MWR radiometer on board SAC-D/Aquarius

Cintia A. Bruscantini, *Student Member, IEEE,* Martin Maas, Francisco Grings, H. Karszenbaum

***Abstract*—The Microwave Radiometer (MWR) on board the SAC-D/Aquarius mission, is a Dicke radiometer operating at 23.8 GHz (H-Pol) and 36.5 GHz (H/V-Pol), which can provide ancillary data for the various retrievals to be performed with Aquarius regarding ocean and land applications. In this study we report calibration results obtained by a land cross-calibration between Windsat and MWR. Moreover, MWR drifts were monitored using Vicarious Cold methodology. Results were generated for the 2011-2012 period using version V5.0S of MWR data.**

MWR and Widsat cross calibration was carried out over selected homogeneous targets which include tropical and boreal forests, desert, grassland and the Sahel. As a result, biases were identified and corrections were proposed.

Drifts in MWR observations were identified by implementing the Vicarious Cold method, which is a statistical approach that estimates the coldest value of the brightness temperature (over ocean) histogram. Time series of such cold values are closely related to drifts in the instrument. In general, it was observed that MWR drifts tend to stabilized within 1K after June 2012, when the software of the on-board computer was updated.

***Index Terms*—MWR; Windsat; cross calibration; vicarious cold.**

I. Introduction

The Microwave Radiometer (MWR) on board the SAC-D satellite was launched in June 2011 [1]. The MWR is a push-broom Dicke radiometer operating at 23.8 GHz (H-Pol) and 36.5 GHz (V- & H-Pol) developed by CONAE, on board the SAC-D. It provides simultaneous spatially collocated measurements with Aquarius observations with the objective of supplying ancillary parameters for Aquarius algorithms. MWR channel 36.5 GHz V-Pol observations over land are useful to estimate canopy temperature [2].

Data products quality are highly related to the radiometric accuracy of the system. In general, biases on retrieved geophysical products can be avoided with accurate calibration of radiometric observations. One technique used in previous satellite missions [3], [4], [5], [6] for on-orbit calibration of microwave radiometers is the cross calibration between two similar instruments over homogeneous extended targets. Cross calibration allows one to identify, quantify and correct calibration offsets that are stable in both space and time, provided that the instrument used as reference is well calibrated.

The methodology relies on the temporal stability of the selected targets and their homogeneity in terms of brightness temperature (Tb), so that radiometers with similar characteristics (frequency, polarization, incidence angle) should observe the same Tb when passing over the target within a short temporal window. Differences in observed Tbs are associated with improper radiometric calibration of the instrument under study and corrected with an adjustment. In this work, MWR cross calibration is performed exploiting the currently on-orbit well-calibrated radiometer Windsat, a Naval Research Laboratory's multi-frequency polarimetric microwave radiometer on board the Coriolis satellite [7]. Coriolis and Aquarius/SAC-D have similar orbital and instrument characteristics (see Table I), which simplifies the inter-calibration between MWR and Windsat. Moreover, it results in temporal collocation of less than 90 minutes in the majority of the cases.

Previous cross calibration of both radiometers has been proposed by [8]. However, the analysis was particularly focused on ocean targets, and therefore in the lowest part of the dynamic range of the radiometer observations ($Tb < 200K$). Furthermore, ocean targets are not as stable as land targets, hence longer temporal windows can be used when calibrating over land sites. In particular, highly stable land targets were found over the world for their use in cross calibration [9]. Such targets include tropical forests, deserts and land ice. Examination of the Tb over these sites and inter-comparison of MWR and Windsat observations in a short period of time over a short time window makes possible the adjustment of MWR Tb to Windsat Tb.

As part of ongoing efforts for MWR calibration, vicarious cold algorithm was implemented to MWR datasets. The Vicarious cold methodology, first proposed by Ruf in [10], seeks to track the coldest Tb values, which presumably occur at calm cold ocean water but at unknown locations. Therefore this theoretical coldest value has to be statistically inferred by processing histograms of the instrument's data.

Section II briefly describes both MWR and Windsat instrument and data, the calibration targets and the Vicarious Cold methodology. In Section III, results of the cross calibration and Vicarious Cold are presented. Correction coefficients derived from the cross calibration are provided. Residues obtained after applying the correction are analyzed. In this Section, MWR temporal drifts in Tb are also shown for each beam and channel. Finally, results obtained are summarized and discussed.

II. Data Sets and Methods

A. MWR

The MWR instrument consists of three Dicke push-broom radiometers on board the SAC-D satellite. MWR has aft- & fore-looking multibeam antennas (8 beams) operating at 23.8 GHz and 36.5 GHz (V- and H-pol) respectively (see

Authors are with the Instituto de Astronoma y Fsica del Espacio (IAFE, CONICET-UBA), C1428ZAA, Argentina (e-mail: cintiab@iafe.uba.ar).

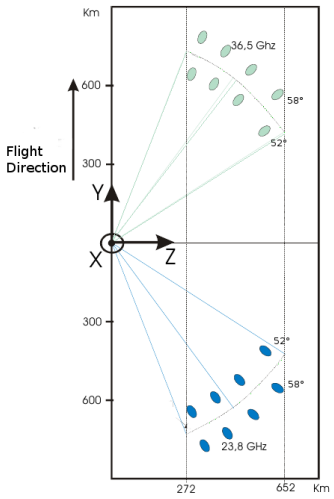

Fig. 1. MWR footprints geometry.

	Windsat	**MWR**
Frequency	23.8 GHz (VH) 37.0 GHz (Polarimetric)	23.8 GHz (H) 36.5 GHz (VH)
Incidence angle	53°	52° & 58°
Instantaneous field of view	12x20 (23.8 GHz) 8x13 (37 GHz)	47.2x29.1 km (52°) 61.7x32.7 km (58°)
Orbit	Sun-synchronous height: 840 km 6 pm ascending time inclination: 98.7° eccentricity: 0.00134	Sun-synchronous height: 657 km 6 pm ascending time inclination: 98.01° eccentricity: 0.0012

TABLE I: MWR & Windsat Characteristics

Fig. 1). The 23.8 GHz channel is only horizontally polarized, while the 36.5 GHz channels measure vertical and horizontal polarized signals. All radiometers resolution is around 40 km on ground. MWR maps the globe in a 7-day revisit period, and its primary goal is to provide ancillary information for Aquarius instrument, NASA's Aquarius instrument on board SAC-D.

The MWR data set used is MWR L1B version 5.0S in both ascending (ASC) and descending (DESC) passes for the period from August 2011 to September 2012.

B. Windsat

Windsat is a conical scanning radiometer on board the Naval Research Laboratory satellite Coriolis, launched on January 6, 2003. Windsat instrument consists of an 11 feed-horn array operating at five frequencies: 6.8, 10.7, 18.7, 23.8 and 37 GHz. The Windsat data set used is HiRes SDR in both ASC and DESC passes aft- & fore-looking for the period from August 2011 to September 2012. Data set was provided by the United States Naval Research Laboratory.

C. Land Cross calibration of MWR and Windsat

MWR L1B brightness temperature at 23.8 GHz channel (Tb23H) and 36.5 GHz channel, V-pol (Tb37V) and H-pol (Tb37H), were compared with Windsat Tb at 23.8 GHz and 37 GHz. Each MWR channel was inter-compared with their corresponding Windsat channel in terms of frequency and polarization. Both instruments observations are contrasted only when measurements are collocated over the targets under study. Ideally, collocation between satellites occurs when the instruments observe near-simultaneously the same target, with the same viewing geometry and the same spectral responses. Simultaneity is desired so that Tb of the target is precisely identical when both instruments make the measurements. However, these conditions are impossible to occur in reality mainly due to orbital constraints. Therefore, temporal thresholds are defined, e.g., a time tolerance for which target Tb should remain stable.

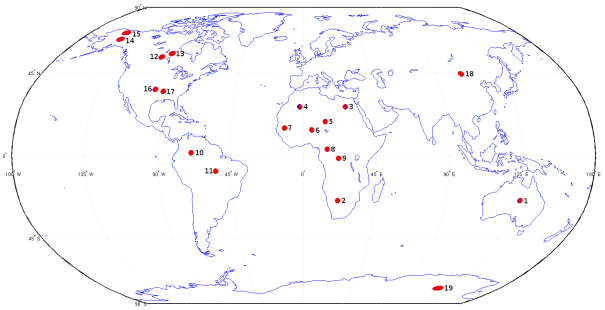

Fig. 2. Location of targets selected for cross calibration over land.

Given the stability of land targets selected and that most of the collocation are expected to occur within 90 minutes (due to MWR-Windsat similar orbital characteristics), a daily time window was used for operational purpose. Due to the instruments' relatively low spatial resolution and the necessity of calibrating with homogeneous targets, areas spanning hundreds of square kilometers were selected. Regarding corrections for incidence angle, none were applied to MWR nor Windsat Tbs owing to closeness of their incidence angles (52° and 58°; and 53° respectively). This is due to the fact that these small differences in observation angle should have a negligible effect on the measured Tb for most targets. In [11], historically incidence angles between 50° and 55° were compared. According to the authors, for vegetated surfaces this incidence angle difference is not expected to make a significant impact, and for bare surfaces it can produce a maximum bias of 1 K.

As a result of the Tbs inter-comparison, a linear adjustment is finally applied to MWR data, customized for each of MWR 8 beams, 3 channels, and for ASC and DESC passes. The adjustment is of the form:

$$Tb_{new}^{MWR} = aTb_{old}^{MWR} + b \quad (1)$$

This correction of L1B MWR data intents to modify MWR Tb values to match Windsat Tbs.

1) Calibration Targets: In order to examine the entire dynamic range of land observations, 19 diverse homogeneous targets were selected, which had been previously used for quality assessment of AMSR-E data [9], including tropical and boreal forests (dense vegetation), deserts and ice land (bare soil), grassland and the Sahel (low vegetation).

Figure 2 shows a global map with the location of the selected targets and their extent marked in red. A detailed list of the selected targets center coordinates with the corresponding numbering can be found in [9]. Areas of the selected target are small (hundreds of square kilometers) compared to the instruments' IFOVs (Instantaneous Field of View) to favor spatial homogeneity. As a consequence, there are sites that are observed by a reduced number of MWR beams. However, given the number of targets selected, this is not a limiting factor, and all the land dynamic range was covered for all MWR beams.

In each site, daily mean and standard deviation of Tb23H, Tb37H and Tb37V were computed for each Windsat and MWR beam and channel, for ASC and DESC passes separately. The cross calibration was performed using averaged Tb values over the red areas extensions to minimize the effect of MWR and Windsat different IFOV sizes.

The homogeneity of the land targets was evaluated by computing the standard deviation of the Tb values of the footprints that were within the target extension for each overpass independently. In general, standard deviations of less than 1K was observed, except for grassland areas and boreal forests where standard deviation may increase in some occasional dates related to rain events. To assess temporal stability, the spatially-averaged Tb time series of Windsat were analyzed. Areas such as Mitu, Salonga, Boumba, and Curua, have an annual Tb dynamic range lower than 5K. Grasslands such as Little Washita or Toolik lake, present a cyclical behavior related to vegetation. However, in these cases, the temporal change rate is slow without significant peaks. It is crucial for the target Tb to remain temporally stable over the collocation time window period considered. In particular, it was observed that the temporal stability is eventually interrupted by rain events. This is the case of the points that are further apart from the 1:1 line in the cross calibration results (see Fig. 6). In such cases, averaged Tb decreases (MWR Tb, Windsat Tb or both) because of rain. Moreover, the spatial standard deviation increases significantly (more than 10 K), due to rain/drying spatial inhomogeneity.

D. Ocean Vicarious Cold Statistical Methodology

With the objective of identifying and tracking drifts in the calibration of MWR, the ocean vicarious cold methodology was implemented. Its main hypothesis is that the lowest possible brightness temperature value is to be found over calm ocean, and that this cold reference should be stable over time. A statistical method was proposed in [10] in order to track this value, and in the present paper that methodology was closely followed in order to analyze MWR data over a one year period since its launch.

As it was found that continental ice could be actually colder than calm ocean, specially in the 37 GHz V-pol channel, areas such as Greenland, Antarctica and Siberia (where is presumable that continental ice could be present) were manually removed. The remaining data was divided in overlapping time windows of 30 days, and a linear extrapolation of the lowest 10% of the histogram (which effectively excludes all remaining land data) was computed and stored. Different lengths of the sampling window were tested and compared during this analysis. It was found that using larger windows to prepare the data for the linear extrapolation has the same effect of a posteriori window-averaging of the resulting estimates of shorter time windows, which clearly has a smoothing effect but eliminates the possibility of identifying shorter term events.

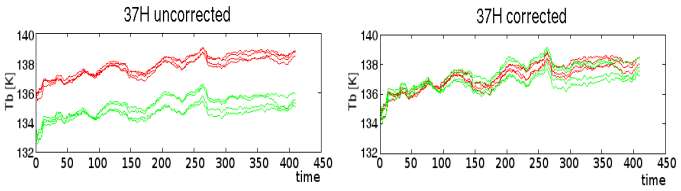

Fig. 3. Incidence angle correction for MWR, 37H channel shown, for odd (red) and even (green) beams.

The present methodology also enables to identify between ASC and DESC passes, by analyzing such data independently. Moreover, in order to compare different beams with each other, an incidence angle correction was performed by a least squares procedure on the resulting cold values (see Fig. 3). At MWR and Windsat incidence angles, Tb might vary between 2K (for H-pol) up to 4 K (V-pol) [12].

III. Results

A. Vicarious Cold

Two different analysis were performed on the resulting cold reference data. First, time series of the cold value for each beam were analyzed and shown in Fig. 4. Results show MWR calibration drifts across all the beams. The data show that, after some initial 10K drifting of beam 7 in 23H channel, the instrument was stabilized after June 2012 to less than 1K drift (in standard deviation) of the computed cold reference value for most of the beams, except for beam 7 in channel 37V. This improvement in the stability of all beams since June 2012 was observed after a new version of the on-board computer software was uploaded.

Also, a general comparison of ASC vs DESC data was performed and it is shown in Fig. 5. The data show an excellent match in the 23 GHz channel, except for beam 7 that shows warmer values for DESC passes. In both 37 Ghz channels, a 1K offset towards warmer DESC values was found, uniformly throughout all beams of the 37H channel and more variable in the 37V, where also beam 7 shows a deviation from this value.

B. MWR & Windsat Tb Inter-Comparison

In this section, results of the MWR and Windsat Tb intercomparison over the 19 selected targets are presented. Moreover, a summary of all the derived linear coefficients is shown in Table II.

1) Tb23H: Figs. 6a and 6d show mean Tb23H values observed by MWR and Windsat for ASC and DESC passes over the 19 homogeneous targets selected. Plots show that the analysis covers most of the system dynamic range likely to be encountered for land Tb (ranging from $\sim 150K$ to

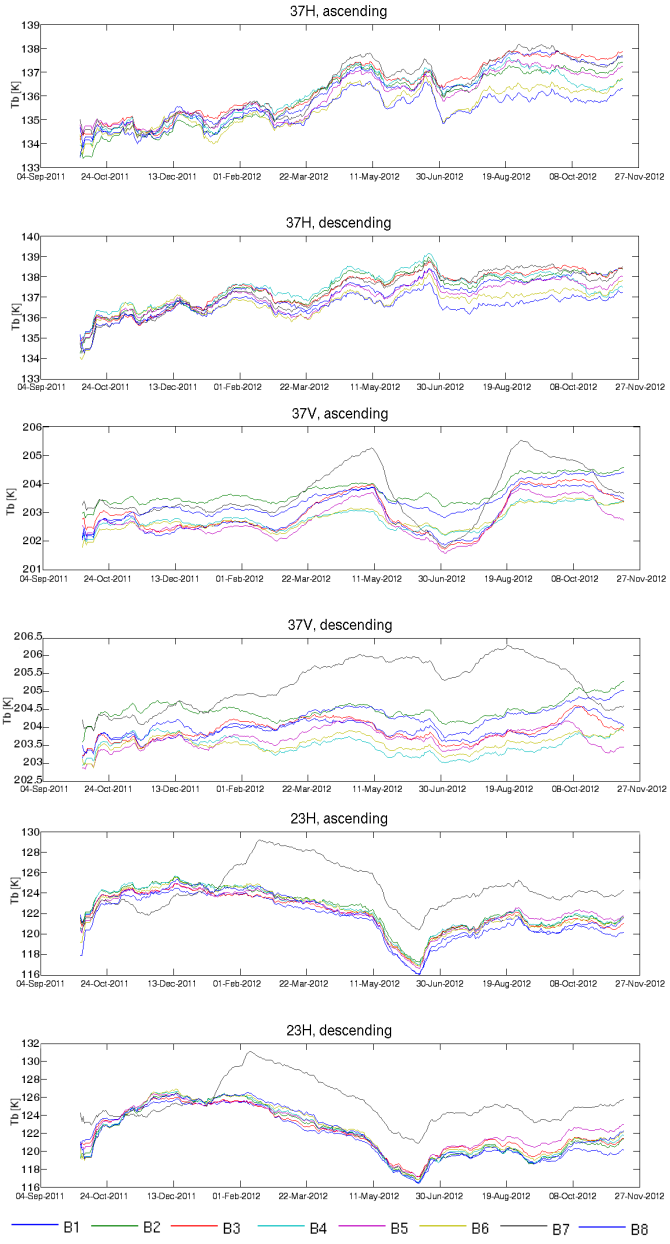

Fig. 4. Time Series of Vicarious Cold Values

$\sim$ $290K$). In general, both instruments' observations are consistent. Nevertheless, lower MWR Tb23H values exhibit a slightly negative bias. Furthermore, in some particular cases, discrepancies between MWR and Windsat Tb values are significant, specially in the ASC case (dots far from the 1:1 line in the plot). However, such observations presented a high standard deviation, most likely associated to rain events. As a result of previous analysis, a minor correction of MWR Tb23H data is expected, in order to increase Tb values of the lowest part of the MWR dynamic range over land and remove the bias found.

2) Tb37H: The same previous analysis was performed for Tb37H and results are shown in Figs. 6b and 6e. In this case, a significant bias was found, that increases as Tb rises. The identified bias becomes appreciable for Tbs higher than $\sim$ $240K$, therefore making it not possible to be noticed on

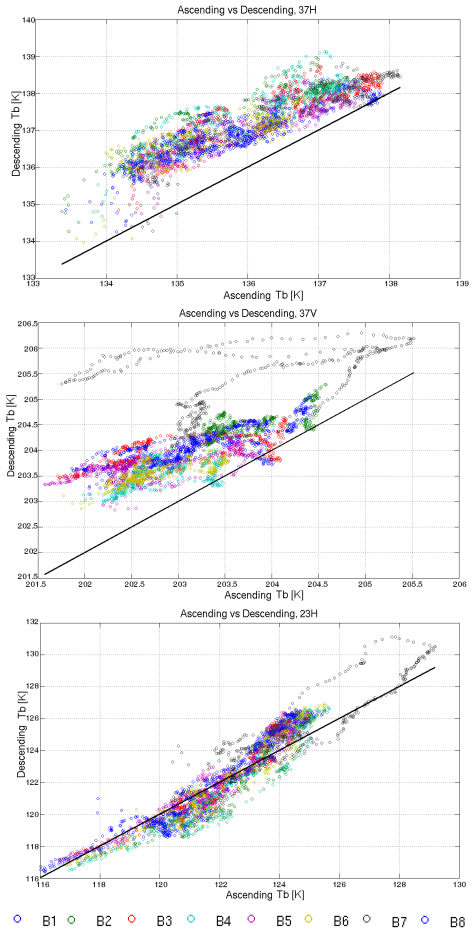

Fig. 5. Vicarious Cold: Ascending vs Descending

previous cross calibration performed by [8] with emphasis over ocean targets (Tbs between $\sim$ $130K$ and $\sim$ $200K$). As MWR Tb37H values are significantly lower than Windsat Tb, linear coefficient "a" on equation (1) for the Tb adjustment is expected to be greater than 1.

3) Tb37V: Figs. 6c and 6f show cross calibration results for Tb37V. MWR Tb exhibits a slight bias. In the cases of high Tb values, MWR observes colder Tb values than Windsat. On the other hand, for low Tb values, MWR overestimates Tb values with respect to Windsat, resulting in a positive bias. Therefore, for Tb37H, "a" values are expected to be greater than 1.

4) Overall Residues: After applying the linear correction to MWR dataset, residues were obtained to check for possible error structure. Residues were calculated as MWR Tb after correction minus Windsat Tb. Results are shown in Fig. 7. Density plots of Windsat Tb vs. residues are shown for the three channels and for ASC & DESC passes. Beam results were not isolated due to similar performance. Nevertheless, ASC and DESC passes yielded different results. In general, ASC passes exhibit a strong nonlinear distribution (dependent on measured Tb), whereas DESC passes do not display such pronounced behavior. Moreover, residues of DESC passes have lower standard deviation. In particular, channels 37H & 37V in the ASC case display a negative residue for Windsat Tb higher than $\sim$ $275K$ and positive residue for lower

Channel	Beam	Ascending		Descending	
		a	b	a	b
23H	1	0.98694	3.9108	0.97297	7.8392
	2	0.8565	39.4745	0.89511	27.123
	3	0.96909	8.2212	0.954	10.5932
	4	0.89756	27.5456	0.92963	19.1245
	5	0.90868	23.2777	1.0008	-0.82069
	6	0.86298	36.4253	0.91648	22.6145
	7	0.93469	16.1957	0.96616	8.1175
	8	0.91447	23.7059	0.93869	16.7805
37H	1	1.1219	-19.1177	1.1383	-24.0788
	2	1.1509	-22.7353	1.1039	-13.6748
	3	1.1286	-21.2954	1.1085	-18.5082
	4	1.0671	-1.9863	1.1053	-13.3515
	5	1.1095	-12.191	1.2475	-45.5736
	6	1.0265	6.0777	1.1215	-16.8013
	7	1.1037	-9.9243	1.1743	-26.4572
	8	1.1038	-11.9025	1.1104	-14.2161
37V	1	1.0591	-14.4051	1.0837	-21.1007
	2	1.1021	-26.5787	1.0795	-21.3856
	3	1.1316	-32.0848	1.0935	-23.8659
	4	1.1007	-24.8229	1.0558	-15.4049
	5	1.1273	-28.7053	1.1553	-37.8758
	6	1.0738	-17.9359	1.0727	-19.2004
	7	1.0318	-8.5096	1.0824	-21.367
	8	1.0638	-16.5852	1.0959	-25.1562

TABLE II: Linear Correction Coefficients

Windsat Tb. On the other hand, 23H ASC exhibits a similar performance, though the residue sign changes at Windsat Tb $\sim 240K$.

IV. Discussion

Calibration and drift monitoring of MWR/SAC-D Tb constitutes an important issue with high impact in all end-users MWR products, such as rain rate, ice concentration, wind speed, soil temperature and others. In order to provide this information, two analysis were carried out: MWR and Windsat cross calibration over land and ocean vicarious cold for drift monitoring.

Cross calibration methodology is a useful tool for post launch calibration to identify, quantify and remove relative biases between two instruments. It involves the inter-comparison of collocated observations of two on-orbit instruments. However, calibration accuracy of the monitored instrument depends on the calibration of the reference instrument. In this work, highly confident Windsat Tb [13] was used as a reference data set for calibrating the MWR, CONAE's radiometer on board the SAC-D spacecraft.

Due to selected site's emissivity features and Coriolis and SAC-D orbital characteristics a daily temporal window was used. For the cross calibration, 19 sites were selected as homogeneous stable targets. As seen in Fig. 6, scene Tbs covered most of the dynamic range for the three channels involved in the calibration. Cross calibration revealed and allowed to remove the following artifacts: (i) existence of a slight negative bias at low Tb23H values; (ii) a significant negative bias throughout the Tb37H dynamic range; (iii) a

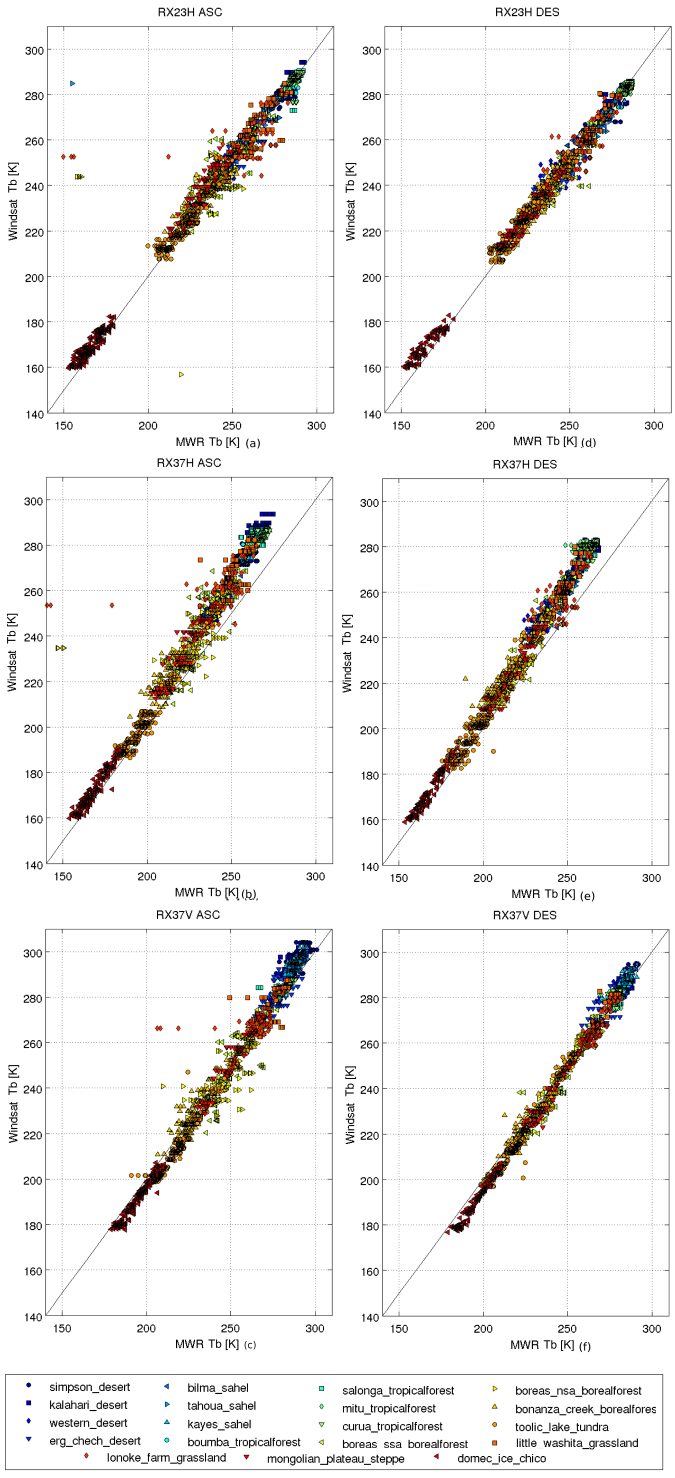

Fig. 6. Cross-calibration of Tb23H, Tb37H, and Tb37V for ASC (a,b,c) and DESC (d,e,f) passes correspondingly.

minor bias in Tb37V, positive at lower Tb values and negative at high ones. In all the cases analyzed (Tb23H, Tb37H and Tb37V), higher Tb values were observed for ASC passes compared to DESC passes. As a result of the analysis, a linear adjustment of MWR Tb was proposed, and calibration coefficients to correct MWR Tbs derived.

Residues after the correction were analyzed. In general, residue of ASC passes exhibited twice the standard deviation

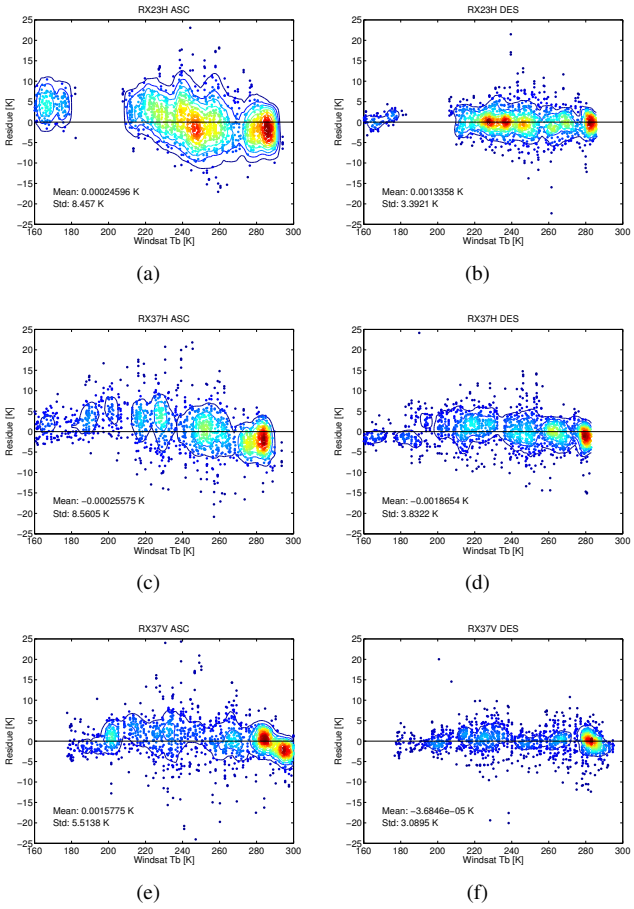

Fig. 7. Density plots of Windsat Tb vs. Residues (*Residue: corrected MWR Tb - Windsat Tb*) for all MWR three channels (RX23H, RX37H & RX37V) for ASC (a,c,e) & DESC (b,d,f) passes correspondingly. Reddish (blueish) markers indicate higher (lower) density distribution of values. Contour lines are plotted in black.

than the one displayed by DESC passes.

Though differences in MWR and Windsat Tb were treated as biases and offsets on MWR radiometric measurements, causes of such biases were not addressed. Further analysis revealed that the main cause of observed bias is the non linearity produced by the square-law detectors of the MWR receivers, and will be corrected in the MWR upcoming data version.

If relative differences between MWR and Windsat observations are not due to MWR calibration errors, it could be argued that they are related to differences on both instruments spectral response, incidence angle and viewing geometry. If this was the case, differences would arise from the collocation methodology itself, thereby introducing artifacts on the corrected data set. Nevertheless, this does not appear to be the case. First, instrument spectral response of both instruments are very similar and the impact is negligible [12]. Second, although different, MWR incidence angles present a 1° and 5° difference (below and above Windsat 53°). Both experimental data and theoretical simulations show that this small difference should have a small effect on measured Tb [11]. Third, due to acquisition strategies (conical scanning vs. push-broom) both instruments can present different viewing angles. However, azimuthal dependence of Tb is very low for these large, homogeneous targets. Finally, all targets and MWR beams displayed consistent results in the linear fit, even for different incidence angles and viewing geometries. Therefore, no systematic bias can be explained only in terms of instrument differences.

Finally, vicarious cold made it possible to examine temporal drifts on each MWR beam and channel in a statistical manner using solely MWR Tb datasets. This allowed to determine a minor drift on ASC and DESC passes of the 37 GHz channels, and to conclude that the initial drifts observed in MWR data were effectively stabilized after June 2012, when the software of the on-board computer was updated.

V. Acknowledgment

This work was funded by MinCyT-CONAE-CONICET SACD/Aquarius Project 12. The authors would like to thank the collaboration of Dr. W. Linwood Jones and his group at the Central Florida Remote Sensing Laboratory and to Lic. Martin Labanda at CONAE.

References

[1] D.M. Le Vine, G. S E Lagerloef, C. Ruf, F. Wentz, S. Yueh, J. Piepmeier, E. Lindstrom, and E. Dinnat, "Aquarius: The instrument and initial results," in *Microwave Radiometry and Remote Sensing of the Environment (MicroRad), 2012 12th Specialist Meeting on*, March 2012, pp. 1–3.

[2] M. Owe and A. A. Van De Griend, "On the relationship between thermodynamic surface temperature and high-frequency (37 ghz) vertically polarized brightness temperature under semi-arid conditions," *International Journal of Remote Sensing*, vol. 22, no. 17, pp. 3521–3532, 2001.

[3] Liang Hong, W. Linwood Jones, and Thomas Wilheit, "Inter-satellite microwave radiometer calibration between amsr and tmi.," in *IGARSS*. pp. 89–92, IEEE.

[4] Liang Hong, W. Linwood Jones, and Thomas Wilheit, "Inter-satellite radiometer calibrations between windsat, tmi and amsr.," in *IGARSS*. 2007, pp. 5240–5243, IEEE.

[5] K. Gopalan, L. Jones, T. Kasparis, and T. Wilheit, "Inter-satellite radiometer calibration of windsat, tmi and ssmi," in *Geoscience and Remote Sensing Symposium, 2008. IGARSS 2008. IEEE International*, July 2008, vol. 2, pp. II–1216–II–1219.

[6] Liyun Dai and Tao Che, "Cross-platform calibration of smmr, ssm/i and amsr-e passive microwave brightness temperature," in *Proc. SPIE*, 2009, vol. 7841, pp. 784103–784103–10.

[7] P.W. Gaiser, K.M. St Germain, E.M. Twarog, G.A. Poe, W. Purdy, D. Richardson, W. Grossman, W.L. Jones, D. Spencer, G. Golba, J. Cleveland, L. Choy, R.M. Bevilacqua, and P.S. Chang, "The windsat spaceborne polarimetric microwave radiometer: sensor description and early orbit performance," *Geoscience and Remote Sensing, IEEE Transactions on*, vol. 42, no. 11, pp. 2347–2361, Nov 2004.

[8] S.K. Biswas, L. Jones, S. Khan, J.-C. Gallo, and D. Roca, "Mwr and windsat inter-satellite radiometric calibration plan," in *Microwave Radiometry and Remote Sensing of the Environment (MicroRad), 2010 11th Specialist Meeting on*, March 2010, pp. 266–271.

[9] Eni G Njoku, T Chan, W Crosson, and A Limaye, "Evaluation of the amsr-e data calibration over land," *Italian Journal of Remote Sensing*, vol. 30, no. 31, pp. 19–37, 2004.

[10] C.S. Ruf, "Vicarious calibration of an ocean salinity radiometer from low earth orbit.," *Journal of atmospheric and oceanic technology*, vol. 20, pp. 1656–1670, 2003.

[11] T. R. H. Holmes, R. A. M. De Jeu, M. Owe, and A. J. Dolman, "Land surface temperature from ka band (37 ghz) passive microwave observations," *Journal of Geophysical Research: Atmospheres*, vol. 114, no. D4, pp. n/a–n/a, 2009, D04113.

[12] T. Meissner and F.J. Wentz, "The emissivity of the ocean surface between 6 and 90 ghz over a large range of wind speeds and earth incidence angles," *Geoscience and Remote Sensing, IEEE Transactions on*, vol. 50, no. 8, pp. 3004–3026, Aug 2012.

[13] W.L. Jones, J.D. Park, S. Soisuvarn, Liang Hong, P.W. Gaiser, and K.M. St Germain, "Deep-space calibration of the windsat radiometer," *Geoscience and Remote Sensing, IEEE Transactions on*, vol. 44, no. 3, pp. 476–495, March 2006.